Monte Carlo Studies of Charmonium and Charmonium Hybrid States

M. Pelizäus, T. Schröder

October 23, 2008

Abstract

In this document MC studies related to the spectroscopy of the charmonium system and the search for predicted charmonium hybrid states are presented. Covered are the production of states falling in the mass range of the charmonium system such as the recently discovered $X(3872)$ and $Y(4260)$ in $\overline{\mathrm{p}}\mathrm{p}$ annihilation in their decays to $J/\psi\eta$, $J/\psi\omega$, and $\psi(2S)\pi^+\pi^-$. Furtheron the production of the predicted spin-exotic charmonium hybrid ground state with an recoiling η meson is studied, where decays to open and hidden charm of the hybrid state are considered.

1 Introduction

One of the goals of the Panda experiment is the precise measurement of the charmonium system and the search for exotic excitations in this mass range. Several states denoted as X, Y and Z have been recently detected, whose nature is controversially debated and which are possibly not conventional charmonium states. The studies described in this document should prove, that these states can be detected with the Panda experiment with sufficient event rates and background suppression. The investigated decay modes include observed decays and predicted decay modes. The latter are important to compare the signature of these states with conventional charmonium states and to reveal their nature.

The studies cover the

- formation of $\eta_c(2S)$, $\psi(2S)$, $X(3872)$ and $Y(4260)$ in their decays to $J/\psi\eta$
- formation of $Y(3940)$ in its decay to $J/\psi\omega$
- formation of $Y(4320)$ in its decay to $\psi(2S)\pi^+\pi^-$
- production of the predicted hybrid ground state ψ_g in $\overline{\mathrm{p}}\mathrm{p} \to \psi_g\eta$ in the decay modes $J/\psi\pi^0\pi^0$ and $D^0\overline{D}^{*0}$ at $\sqrt{s} = 5.473$ GeV

in exclusively reconstructed $\overline{\mathrm{p}}\mathrm{p}$ annihilation events.

In the following general considerations about the signal cross sections and the expected background channels are discussed. Afterwards the anaylsis strategy which is similar for all investigated channels is presented, before the reconstruction and event selection for the individual reactions is described and the obtained results are discussed in separated sections.

1.1 Signal Cross Sections

Due to lack of data in conjecture with missing predictions for charm production in $\overline{\mathrm{p}}\mathrm{p}$ annihilation in the mass range above the $D\overline{D}^*$ threshold, only assumptions can be made for most of the production cross sections of the states under study. In cases where no predictions exist the expected signal yield and signal to background ratio is given in terms of the unknown cross section. For the hybrid state the $\overline{\mathrm{p}}\mathrm{p} \to \psi_g\eta$ cross section is assumed to be the same as for the reaction $\overline{\mathrm{p}}\mathrm{p} \to \psi(2S)\eta$, where the cross section is calculated from the crossed processed $\psi(2S) \to \eta\overline{\mathrm{p}}\mathrm{p}$.

1.2 Background Considerations

The considered background sources for the investigated signal reactions including charmonium resonances can be devided into two classes. In the first category the events include a J/ψ or another charmonium state decaying into J/ψ. The final states could include the same particles as the signal final state, but the decay paths are different. Furtheron events of this class could have a different photon multiplicity than signal events. These two types of events have a similar topology as signal events and could therefore potentially pollute the signal. As

for signal events the cross sections have not been measured in most cases.

Events of the second category do not include a charmonium state and the final states do only have charged or neutral pions. Due to misidentification of a pion pair as a e^+e^- or $\mu^+\mu^-$ pair these events could be a source for background. Their cross sections are expected to be enhanced by several orders of magnitude over the signal cross sections. However, most of the cross sections have not been measured in the energy range of interest. Two methods can be applied to estimate the cross sections. Where measurements exist for a certain reaction at different points in the lower energy region the cross sections are extrapolated towards higher energies. Often the cross section has been measured at only one energy point and an extrapolation is not possible. In these cases the cross sections are extracted from the DPM event generator [**?**] for generic $\overline{\mathrm{p}}\mathrm{p}$ events. The number of generated events having a particular final state is normalized to the total number of generated events and multiplied by the total $\overline{\mathrm{p}}\mathrm{p}$ cross section at the given energy obtained from Ref. [**?**]. As a cross check this method is applied for energies, where measurements exist. Depending on the final state and energy it is found that the cross sections estimated by this method underestimate the measured cross sections by a factor of approximately 3.

For the study of $\overline{\mathrm{p}}\mathrm{p} \to \psi_g\eta$ with ψ_g decaying to open charm only open charm events have been considered, where the cross sections have not been measured either.

1.3 Analysis Strategy

Apart from the considered open charm decay mode of the ψ_g all states under study are decaying directly or via another charmonium state to a J/ψ and one or more associated light mesons. The approach for the reconstruction for these decay pathes is the same: First the J/ψ is reconstructed from its decays to an e^+e^- and $\mu^+\mu^-$ lepton pair. Afterwards J/ψ candidates in an event are combined with light meson resonances or charged pions. The combined candidates are kinematically fitted by constraining the sum of the final state particles' four-vectors to the inital $\overline{\mathrm{p}}\mathrm{p}$ momentum and energy (BC fit). A common vertex for the charged particles is also required. This fit leads to an improvement of the invariant mass resolution of intermediate resonances in the decay tree and allows to apply narrow mass windows on the invariant mass of the resonance candidate for a clean selection. For the final event selection the fit is repeated but applying additional mass constraints on the intermediate resonances when possible, i.e. the intrinsic width of the resonance is narrower than the invariant mass resolution (BM fit). In the case that more than one accepted candidate is found in a given event only the candidate which leads to the highest confidence level (CL) of the BM fit is considered for further analysis.

In the last step of the analysis the signal yield and selection efficiency is determined. Therefore the final fit is repeated but with applying only the mass constraints and removing the constraint on the initial $\overline{\mathrm{p}}\mathrm{p}$ system momentum and energy (M fit). This results in a signal of finite resolution, where the number of reconstructed candidates can be extracted from.

In the following sections the J/ψ reconstruction and the selection of the considered systems following the method delineated above is described in detail. The ψ_g reconstruction from its open charm decay is similar to the approach given above and is addressed in section 7.

2 J/ψ reconstruction

For the reconstruction of the J/ψ decay to an e^+e^- and $\mu^+\mu^-$ lepton pair two particle candidates of opposite charge, both identified as electrons or muons are combined to J/ψ candidates having an invariant mass in the intervall $[2.7; 3.3]$ GeV/c^2. A likelihood based selection algorithm exploiting the information of the MVD, STT, DIRC, EMC and the muon detector is applied for particle identification [**?**]. The likelihood value for one of the candidates of a given e^+e^- pair being identified as an electron or positron should be $\mathcal{L} > 0.85$, whereas the other candidate should fulfill the tighter criteria $\mathcal{L} > 0.99$. In case of the $J/\psi \to \mu^+\mu^-$ decay mode both candidates are required to have a likelihood value greater than 0.85 to be identified as muons.

Accepted J/ψ candidates are kinematically fitted requiring a common vertex for the e^+e^- and $\mu^+\mu^-$ candidates. Only candiates which yield a confidence level of the fit $CL > 0.1\%$ are accepted for further analysis.

These criteria yield in general sufficient rejection of the considered background reactions including two or more charged pions. The situation is distinct for the $J/\psi \to \mu^+\mu^-$ decay mode. It turned out that even the application of the very stringent criteria $\mathcal{L} > 0.85$ to both of the candidates of a given $\mu^+\mu^-$ pair does not suppress these background reactions to the desired level. Thus the results for the decay

$J/\psi \to \mu^+\mu^-$ are reported in this document but are not included in the final results (i.e. the expected signal yield and signal to background ratio) of these studies. Currently the muon detector is undergoing a redesign, which should improve the identification of muons.

3 Study of the $J/\psi\omega$ system

The $Y(3940)$ having a mass of $3943 \pm 11(stat) \pm 13(syst)$ MeV/c^2 and a width of $87 \pm 22(stat) \pm 26(syst)$ MeV/c^2 has been observed in the decay mode $J/\psi\omega$ in $B \to Y(3940)K$ decays by the Belle and Babar collaborations. The quantum numbers of the state are unknown. It is not observed in $D\overline{D}$ or $D\overline{D}^*$ decays. This decay pattern is not in accord with expectations for a charmonium state, where the decay into $J/\psi\omega$ is OZI-suppressed and it has been suggested that the $Y(3940)$ is exotic. Exotic interpretations include a charmonium hybrid state, a multiquark state or a molecule state.

In the following an inclusive study of the formation of $Y(3940)$ in $\overline{\mathrm{p}}\mathrm{p}$ annihilation is presented. The J/ψ is reconstructed from its decays to e^+e^- and $\mu^+\mu^-$, whereas the ω is reconstructed via the $\pi^+\pi^-\pi^0$ decay mode.

3.1 Background Considerations

As possible sources of background the reactions

- $\overline{\mathrm{p}}\mathrm{p} \to \psi(2S)\pi^0$ $(\psi(2S) \to J/\psi\pi^+\pi^-)$
- $\overline{\mathrm{p}}\mathrm{p} \to J/\psi\rho^0\pi^0$ $(\rho^0 \to \pi^+\pi^-)$
- $\overline{\mathrm{p}}\mathrm{p} \to J/\psi\rho^+\pi^-$ $(\rho^+ \to \pi^0\pi^+)$
- $\overline{\mathrm{p}}\mathrm{p} \to \pi^+\pi^-\pi^0\rho^0$ $(\rho^0 \to \pi^+\pi^-)$
- $\overline{\mathrm{p}}\mathrm{p} \to \pi^+\pi^-\pi^-\rho^+$ $(\rho^+ \to \pi^0\pi^+)$
- $\overline{\mathrm{p}}\mathrm{p} \to \pi^+\pi^-\omega$ $(\omega \to \pi^+\pi^-\pi^0)$

have been considered.

None of the cross sections for these reactions have been measured in the energy range of the $Y(3940)$. The cross sections for the reactions $\overline{\mathrm{p}}\mathrm{p} \to \pi^+\pi^-\pi\rho$ and $\overline{\mathrm{p}}\mathrm{p} \to \pi^+\pi^-\omega$ have been measured in the $\sqrt{s}$ energy range between 2.14 and 3.55 GeV [**?**]. They are shown in Fig. 1 in dependence of $\sqrt{s}$. The data can be fitted by an exponential function $\sim \exp(-s)$ and the cross section at $\sqrt{s} = 3.94$ GeV is estimated by extrapolating this function. The obtained values are presented in Table 1. In addition the cross sections are extracted from the DPM event generator

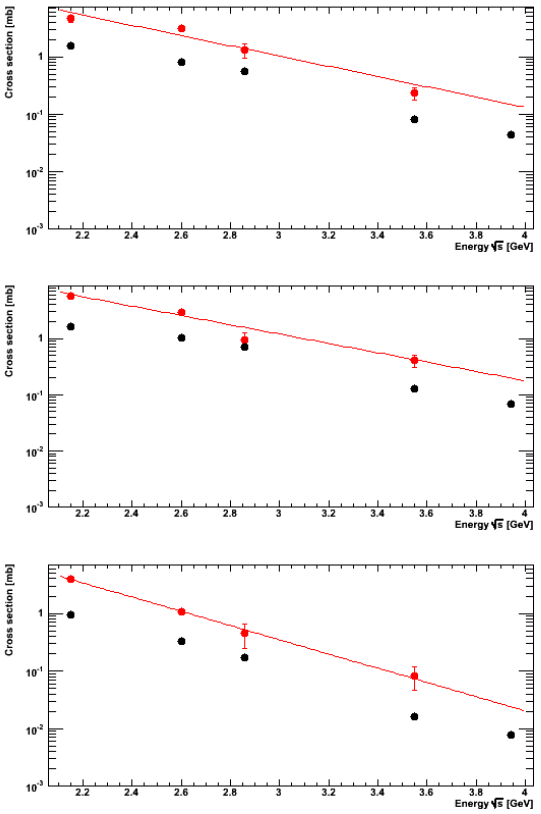

Figure 1: Cross sections for the reactions a) $\overline{\mathrm{p}}\mathrm{p} \to \pi^+\pi^-\pi^0\rho^0$, b) $\overline{\mathrm{p}}\mathrm{p} \to \pi^+\pi^-\pi^-\rho^+$ and c) $\overline{\mathrm{p}}\mathrm{p} \to \pi^+\pi^-\omega$ in dependence of $\sqrt{s}$. The measured cross sections (red dots) are overlaid by the result of the fit using a function $\sim \exp(-\sqrt{s})$, which is applied to extrapolate the cross section towards $\sqrt{s} = 3.94$ GeV. Also shown are the cross sections derived from the DPM event generator (black).

applying the technique described above. The results are shown in Fig. 1 together with data. The extracted cross sections from the generator underestimate the data over the hole energy range. At $\sqrt{s} = 3.94$ GeV the extracted values are ≈ 3 times lower than the values derived from extrapolating the fit function. The reason for the observed deviation is not known and needs further investigation. However, in this study the values derived from the extrapolation are applied.

For the channels including charmonium states one has to distinguish between the formation process $\overline{\mathrm{p}}\mathrm{p} \to Y(3940)$ followed by the subsequent $Y(3940)$ decay on the one hand and direct production of a charmonium state with an associated recoil meson on the other hand. While the observed decay of the $Y(3940)$ into $J/\psi\omega$ is considered to be iso-spin conserving, a decay into $\psi(2S)\pi^0$ is iso-spin violating and thus expected to be suppressed. Here

Reaction $\overline{\mathrm{p}}\mathrm{p} \to$	Cross section at $\sqrt{s} = 3.94$GeV Extr. $[\mu b]$	DPM $[\mu b]$
$\pi^+\pi^-\pi^0\rho^0$	149	43.3 ± 1.9
$\pi^+\pi^-\pi^0\rho^+$	198	67.7 ± 2.3
$\pi^+\pi^-\omega$	23.9	7.87 ± 0.8

Table 1: Cross sections for the background reactions under study. Listed are the values obtained from the extrapolation of measurements in the $\sqrt{s}$ range 2.15 – 3.55 GeV and the corresponding values extracted from the DPM generator.

Reaction $\overline{\mathrm{p}}\mathrm{p} \to$	σ	$\mathcal{B}$
$Y \to J/\psi\omega$	σ_S	$10.4\% \times \mathcal{B}(Y \to J/\psi\omega)$
$\pi^+\pi^-\pi^0\rho^0$	$149\,\mu b^*$	100%
$\pi^+\pi^-\pi^-\rho^+$	$198\,\mu b^*$	100%
$\pi^+\pi^-\omega$	$23.9\,\mu b^*$	100%
$\psi(2S)\pi^0$	55 pb	3.73%
$Y \to J/\psi\rho\pi$	σ_S	$11.7\% \times \mathcal{B}(Y \to J/\psi\rho\pi)$

Table 2: Cross sections for signal and background reactions. The table lists also the branching ratios for the subsequent particle decays. The cross sections marked by an asterisk ($*$) take already the branching ratios of subsequent particle decays into account and the corresponding branching ratios are listed therefore as 100%.

the non-resonant reaction $\overline{\mathrm{p}}\mathrm{p} \to \psi(2S)\pi^0$ is considered as a possible source of background. Ref. [**?**] quotes the cross section for this process to be less than 55 pb. In this study a value of 55 pb is assumed for this process as a conservative estimate. Background could also arise from hypothetical isospin conserving $Y(3940)$ decays into $J/\psi\rho\pi$, with a possible intermediate resonance decaying into $\rho\pi$. Since the time-scales of the two processes are distinct, less interference between the final states is expected and the background is considered to be incoherent to signal. For the branching fractions of the $Y(3940)$ into $J/\psi\rho^0\pi^0$ and $J/\psi\rho^+\pi^-$ a ratio of 1 : 2 is assumed, a decay pattern which is expected for a iso-scalar state.

Table 2 summarizes the assumed cross sections and the branching fractions of the signal and background reactions under study.

3.2 Data samples

The number of analyzed signal and background events is summarized in Table 3. Signal events have been generated with phase space distribution for the reaction $Y(3940) \to J/\psi\omega$. For the

Reaction $\overline{\mathrm{p}}\mathrm{p} \to$	Events	Filter eff.
$J/\psi\omega$	$4 \cdot 10^4$	100%
$\pi^+\pi^-\pi^0\rho^0$	$5 \cdot 10^6$	0.77%
$\pi^+\pi^-\pi^-\rho^+$	$5 \cdot 10^6$	0.81%
$\pi^+\pi^-\omega$	$1 \cdot 10^7$	9.15%
$J/\psi\pi^-\rho^+$	$5 \cdot 10^5$	100%
$J/\psi\pi^0\rho^0$	$5 \cdot 10^5$	100%
$\psi(2S)\pi^0$	$2 \cdot 10^5$	100%

Table 3: Summary of analyzed events and the J/ψ mass filter efficiency. For channels including charmonium states no filter is applied and the J/ψ is decaying to e^+e^- and $\mu^+\mu^-$ with equal branching fraction of 50%.

$\omega \to \pi^+\pi^-\pi^0$ a proper angular distribution is considered (OMEGA_DALITZ decay model from EvtGen event generator)[**?**]. The background reactions $\overline{\mathrm{p}}\mathrm{p} \to \pi^+\pi^-\omega$ and $\overline{\mathrm{p}}\mathrm{p} \to \pi^+\pi^-\pi\rho$ require a large amount of data. To simulate the demanded number of events within a sufficient time the J/ψ mass filter technique as described in App. A is applied and the number of events analyzed for these reactions has to be corrected by the filter efficiency, which is also listed in Table 3.

3.3 Event Selection

The $J/\psi\omega$ system is reconstructed by combining the J/ψ candidates found in an event with $\omega \to \pi^+\pi^-\pi^0$ candidates. To form the latter, two candidates of opposite charge, both identified as pions having a likelihood value $\mathcal{L} > 0.2$ are combined together with $\pi^0 \to \gamma\gamma$ candidates, composed from two photon candidates having an invariant mass in the range $[115; 150]$ MeV/c^2.

All combinations of an event are fitted by constraining the sum of the four-momenta of the final state particles to the inital beam energy and momentum and constraining the origin of the charged final state particles to a common vertex. Combinations where the fit yields a confidence level less than 0.1% are not considered for further analysis. The invariant mass of the J/ψ and ω candidates obtained after the fit are shown in **??**. The J/ψ and ω signal have a FWHM of 9 MeV/c^2 and 16.5 MeV/c^2, respectively. A ω mass window of $[750; 810]$ MeV/c^2 is applied to cleanly select $J/\psi\omega$ candidates. For the final event selection the accepted candidates are fitted under the $J/\psi\omega$ hypothesis, where on top of the $\overline{\mathrm{p}}\mathrm{p}$ four-momentum constraint mass constraints are applied to the J/ψ and π^0 candidates. Only candidates where the fit yields a confidence level $CL > 0.1\%$

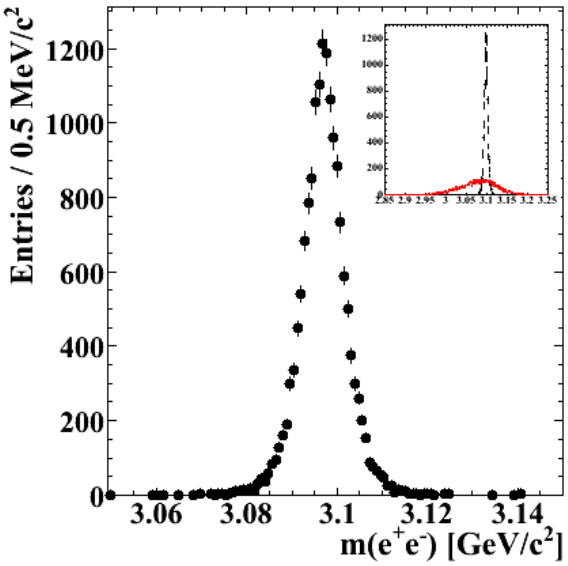

Figure 2: Invariant $J/\psi \to e^+e^-$ mass obtained after the kinematic fit of $J/\psi\omega$ candidates applying the constraints on the inital $\overline{\mathrm{p}}\mathrm{p}$ four-momentum. The inset shows the same signal (black) compared to the distribution obtained before the fit (red) in an extended mass region.

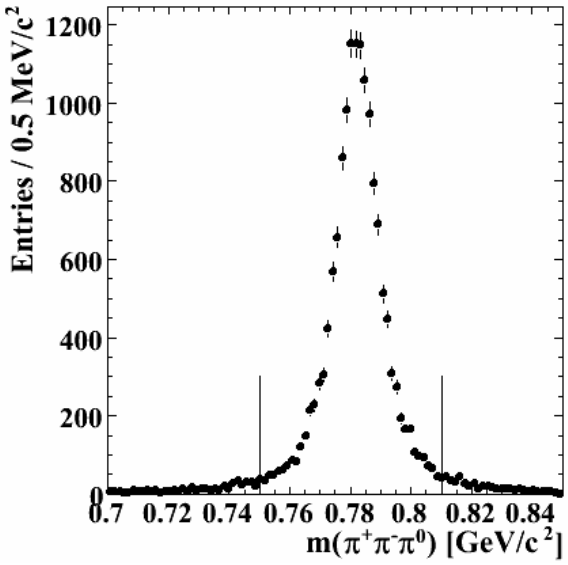

Figure 3: Invariant $\pi^+\pi^-\pi^0$ mass obtained after the kinematic fit of $J/\psi\omega$ (with $J/\psi \to e^+e^-$) candidates with constraints on the inital $\overline{\mathrm{p}}\mathrm{p}$ four-momentum. The ω mass window applied for selection is indicated by the vertical lines.

are considered furtheron.

To supppress background arising from $\overline{\mathrm{p}}\mathrm{p} \to \psi(2S)\pi^0$ reactions events are rejected, where the invariant $J/\psi\pi^+\pi^-$ mass of the $J/\psi\omega$ candidates falls into to the intervall $[3.6725; 3.7]$ GeV/c^2 around the $\psi(2S)$ mass. The invariant $J/\psi\pi^+\pi^-$ mass is shown in Fig. 4 for signal and background events.

At this stage of the analysis in 0.14% of the analyzed signal events more than one $J/\psi\omega$ candidate is found. The ambiguity is solved by selecting the combination in the event which is leading to the highest confidence level for the fit assuming the $J/\psi\omega$ hypothesis. In 60% of the cases the selected combination is corresponding to the generated combination and thus is the correct one. In total a negligible fraction of $5.5 \cdot 10^{-4}$ out of the signal events is reconstructed in the wrong combination.

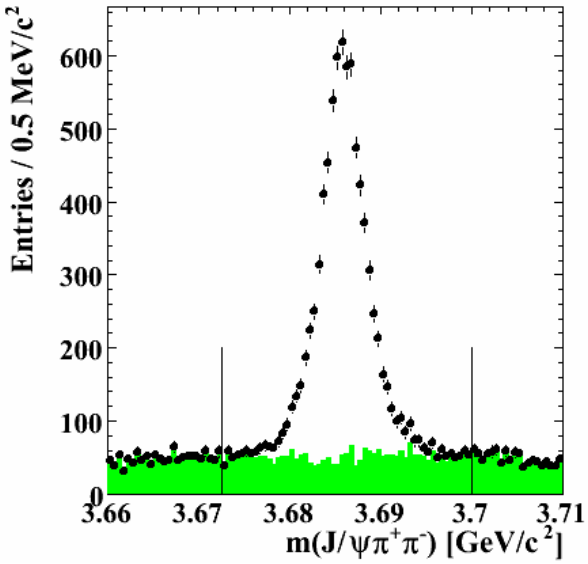

Figure 4: Invariant $J/\psi\pi^+\pi^-$ ($J/\psi \to e^+e^-$) mass of the accepted $J/\psi\omega$ candidates for signal and $\psi(2S)\pi^0$ background events. The background distribution is shown on top of the signal distribution (shaded) and is normalized to the signal cross section and branching fraction according to Table 2. The vertical lines indicate the mass region used for the $\psi(2S)$ veto.

3.4 Results

The reconstruction efficiency is estimated separately for events reconstructed via the two different J/ψ decay modes. Only the correct combinations are considered. The efficiency is found to be 13.2% ($J/\psi \to e^+e^-$) and 12.6% ($J/\psi \to \mu^+\mu^-$).

The invariant $J/\psi\omega$ mass distribution obtained from a kinematic fit similar to the final fit applying the

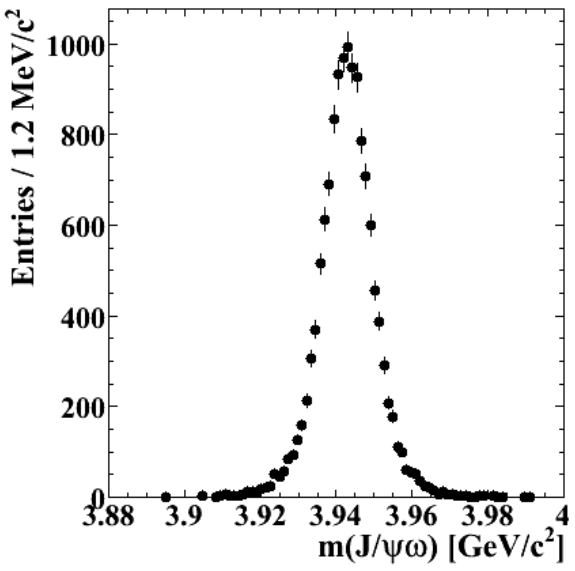

Figure 5: Invariant $Y(3940) \to J/\psi\omega$ mass distribution obtained after the kinematic fit applying the constraints described in the text.

J/ψ and π^0 mass constraints, but removing the constraint on the beam momentum and energy is shown in Fig. 5. The signal width (FWHM) is found to be 14.4 MeV/c^2.

In order to estimate the pollution of the signal from the considered background reactions, background events are analyzed likewise as signal events and the number of reconstructed $J/\psi\omega$ candidates is determined. The suppression η for a certain background reaction is defined as the fraction of generated and accepted events and is given in Table 4 for the individual background channels. The expected signal to noise ratio is then given by

$$\frac{S}{N} = \frac{\sigma_S}{\sigma_B}\,\frac{\mathcal{B}_S}{\mathcal{B}_B}\,\frac{\epsilon}{\eta^{-1}}, \qquad (1)$$

where σ_s (σ_B) is the cross section and $\mathcal{B}_S$ ($\mathcal{B}_B$) is the product of branching fractions for signal (background) reactions, and ϵ is the signal reconstruction efficiency. Since the cross section σ_S and the branching fraction $\mathcal{B}(Y \to J/\psi\omega)$ for the signal process $\overline{\mathrm{p}}\mathrm{p} \to Y \to J/\psi\omega$ is not known the signal to noise ratio is reported with respect to the product $\tilde{\sigma} = \sigma_S\mathcal{B}(Y \to J/\psi\omega)$. Table 4 summarizes the expected ratio S/N together with the derived suppression for the various background reactions.

A very good background suppression better than $6 \cdot 10^8$ and $1 \cdot 10^8$ is achieved for the channels $\overline{\mathrm{p}}\mathrm{p} \to \pi^+\pi^-\pi\rho$ and $\overline{\mathrm{p}}\mathrm{p} \to \pi^+\pi^-\omega$, respectively if the J/ψ is reconstructed from its e^+e^- decay mode. Here the expected signal to noise ratio is better than $21 - 31\tilde{\sigma}/nb$, depending on the background channel. If the $J/\psi \to \mu^+\mu^-$ decay mode is considered a background suppression in the order of 10^5 ($\overline{\mathrm{p}}\mathrm{p} \to \pi^+\pi^-\omega$) and 10^7 ($\overline{\mathrm{p}}\mathrm{p} \to \pi^+\pi^-\pi\rho$) is obtained, yielding a S/N of $0.08\tilde{\sigma}/\,\mathrm{nb}$ and $1.7\tilde{\sigma}/\,\mathrm{nb}$ respectively. The first ratio is insufficient and the separation of muons and pions has to be clearly improved before the $J/\psi \to \mu^+\mu^-$ channel becomes measureable.

For the $\psi(2S)\pi^0$ background a S/N of $6.15\tilde{\sigma}/\,\mathrm{pb}$ ($J/\psi \to e^+e^-$) and $16.3\tilde{\sigma}/pb$ ($J/\psi \to \mu^+\mu^-$) is yielded. Thus the expected signal pollution is very low. For the two $J/\psi\rho\pi$ channels a suppression by an order of magnitude is observed and the expected S/N for the sum of the two $J/\psi\rho\pi$ charge combinations is $2.81\mathcal{BR}$ ($J/\psi \to e^+e^-$) and $3.05\mathcal{BR}$ ($J/\psi \to \mu^+\mu^-$), where $\mathcal{BR} = \mathcal{B}(Y \to J/\psi\omega)/\mathcal{B}(Y \to J/\psi\rho\pi)$.

Both reactions can be disentangled performing a partial wave analysis, which is out of the scope of this document. However, it should be noted that the $\omega \to \pi^+\pi^-\pi^0$ decay has a distinct angular distribution from the decay $\rho\pi$ with $\rho \to \pi\pi$. The ω helicity angle θ_h is defined as the angle between the π^+ and π^0 momentum computed in the $\pi^+\pi^-$ center of mass system. For signal events the $\cos\theta_h$ distribution is $\sim \sin^2\theta_h$. The reconstructed θ_h distribution for signal and background events is shown in Fig. 6 together with the reconstruction efficiency in dependence of $\cos\theta_h$. The efficiency distribution shows no prominent structures and is homogeneous with respect to statistical uncertainties. A linear fit to the efficiency distribution yields a gradient consistent with zero within statistical errors. Thus the angle θ_h can be cleanly reconstructed without significant distortion due to an inhomogeneity of the efficiency. The $\cos\theta_h$ distribution reconstructed from signal events shows the expected $\sim \sin^2\theta_h$ dependence, which is distinct from the distribution obtained for background events. The result for background events is derived assuming a phase space distribution for the $Y \to J/\psi\rho\pi$ decay. Depending on the production process of the ρ meson its helicity and thus the angular distribution for $\rho \to \pi\pi$ can vary. The two scenarios where the ρ decay angle is $\sim \sin^2$ and $\sim \cos^2$ have been tested by weighting the generated events accordingly. The observed θ_h distributions are independent of the assumed $\rho \to \pi\pi$ angular distribution. In conclusion it is expected that the $J/\psi\omega$ and $J/\psi\rho\pi$ decay modes could be disentangled performing a partial wave analysis of the $J/\psi\pi^+\pi^+\pi^0$ final state.

Since the reconstruction via the channel $J/\psi \to \mu^+\mu^-$ yields not a sufficient background suppression

Reaction	$\eta_{e^+e^-}$	$\eta_{\mu^+\mu^-}$	$S/N_{e^+e^-}$	$S/N_{\mu^+\mu^-}$
$\pi^+\pi^-\pi^0\rho^0$	$> 6.49 \cdot 10^8$	$3.82 \cdot 10^7$	$> 29.9\,\tilde{\sigma}/\,\text{nb}$	$1.68\,\tilde{\sigma}/\,\text{nb}$
$\pi^+\pi^-\pi^-\rho^+$	$> 6.16 \cdot 10^8$	$2.20 \cdot 10^7$	$> 21.4\,\tilde{\sigma}/\,\text{nb}$	$0.75\,\tilde{\sigma}/\,\text{nb}$
$\pi^+\pi^-\omega$	$> 1.08 \cdot 10^8$	$2.89 \cdot 10^5$	$> 31.6\,\tilde{\sigma}/\,\text{nb}$	$0.079\,\tilde{\sigma}/\,\text{nb}$
$\psi(2S)\pi^0$	$1.8 \cdot 10^3$	$5 \cdot 10^3$	$6.15\,\tilde{\sigma}/\,\text{pb}$	$16.3\,\tilde{\sigma}/\,\text{pb}$
$J/\psi\pi^-\rho^+$	25	28.3	$4.40\,\mathcal{BR}$	$4.75\,\mathcal{BR}$
$J/\psi\pi^0\rho^0$	22	25.2	$7.74\,\mathcal{BR}$	$8.47\,\mathcal{BR}$

Table 4: Observed background suppression η and the expected signal to noise ratio S/N for the investigated background reactions listed separately for J/ψ reconstructed from the e^+e^- and $\mu^+\mu^-$ decay mode. The ratio S/N is reported for $Y \to J/\psi\pi\rho$ with respect to the unknown ratio $\mathcal{BR} = \mathcal{B}(Y \to J/\psi\omega)/\mathcal{B}(Y \to J/\psi\rho\pi)$ of the branching fractions for the reations $\overline{\text{p}}\text{p} \to Y \to J/\psi\omega$ and $\overline{\text{p}}\text{p} \to Y \to J/\psi\rho\pi$.

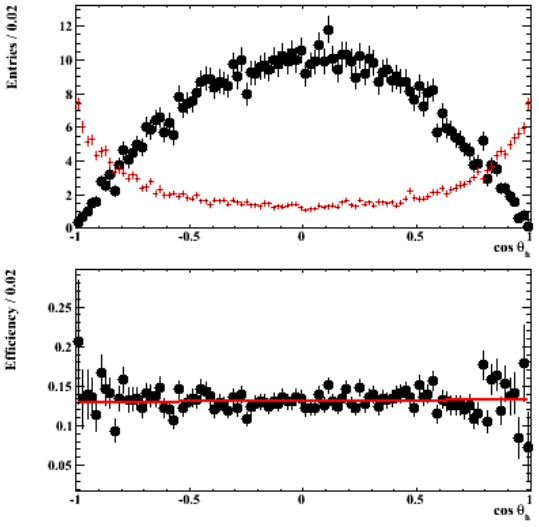

Figure 6: Distribution of the helicity angle θ_h (top) for signal (black) and $\overline{\text{p}}\text{p} \to J/\psi\rho\pi$ background (red) events. The distributions are normalized to the branching fraction $\mathcal{B}(Y \to J/\psi\omega)$ and $\mathcal{B}(Y \to J/\psi\rho\pi)$, respectively. Also shown is the reconstruction efficiency in dependence of θ_h (bottom). The red line is the result of a fit using a linear function.

for $\overline{\text{p}}\text{p} \to \pi^+\pi^-\omega$, the analysis is restricted to the $J/\psi \to e^+e^-$ decay mode only. The number of reconstructed events per day running the accelerator at the $Y(3940)$ peak position and design luminosity of $\mathcal{L} = 2 \cdot 10^{32}\text{cm}^{-2}\text{s}^{-1}$ is given by

$$N = \epsilon_S \tilde{\sigma} \int \mathcal{L}\text{d}t = 119\tilde{\sigma}\ \text{nb}^{-1}. \qquad (2)$$

4 Study of the $J/\psi\eta$ system

The $J/\psi\eta$ final state is examined for four different beam momenta, allowing to study the formation of the resonances $\eta_c(2S)$, $\psi(2S)$, $X(3872)$ and $Y(4260)$ in $\overline{\text{p}}\text{p}$ annihilation events. For each signal mode, the contributions of different background modes are investigated (Table 12). The analysis uses release 0.15.10 where the EMC edge correction is integrated **??**.

The $\psi(2S)$ and the $\eta_c(2S)$ are charmonium states. The $\eta_c(2S)$ was discovered by Belle and has been studied recently in 2-photon production by BABAR and CLEO. Its mass is currently given with 3637 ± 4 MeV/c^2 and its width with 14 ± 7 MeV/c^2.

The classification of the other two states is still an open question, including missing $c\bar{c}$ states, molecules, tetraquarks and hybrid states. The X(3872) has a mass of 3872.2 ± 0.8 MeV/c^2 and a width of $3.0 \pm 1.7 \pm 0.9$ MeV/c^2. It has been observed in the decay to $J/\psi\pi^+\pi^-$ in $B^+ \to X(3872)K^+$ by Belle. Possible quantum numbers based on an angular analysis are 1^{++} and 2^{-+}. The $Y(4260)$ has been observed in the decay to $J/\psi\pi^+\pi^-$ in e^+e^- ISR events at BABAR and CLEO. Its mass is given with 4.26 GeV/c^2, the width with 90 MeV/c^2.

4.1 Background considerations

Possible background modes include

- $\overline{\mathrm{p}}\mathrm{p} \to J/\psi\pi^0\gamma$
- $\overline{\mathrm{p}}\mathrm{p} \to J/\psi\pi^0\pi^0$
- $\overline{\mathrm{p}}\mathrm{p} \to J/\psi\eta\gamma$
- $\overline{\mathrm{p}}\mathrm{p} \to J/\psi\eta\pi^0$
- $\overline{\mathrm{p}}\mathrm{p} \to J/\psi\eta\eta$
- $\overline{\mathrm{p}}\mathrm{p} \to \pi^+\pi^-\eta$
- $\overline{\mathrm{p}}\mathrm{p} \to \pi^+\pi^-\pi^0$

with $\pi^0 \to \gamma\gamma$, $\eta \to \gamma\gamma$, $J/\psi \to e^+e^-$ and $\mu^+\mu^-$.
Most cross-sections for decays including an J/ψ have not been measured yet. The cross-sections of the modes without a J/ψ have been either directly measured 3.1 or are obtained from the DPM generator (section **??**) and are listed in table 12.

4.2 Data samples

The number of generated events for the signal and background studies are listed in Tab. 5. 40000 events have been generated for each of the first three signal modes, and 80000 events for the $Y(4260)$ mode. The J/ψ decays with 50% into e^+e^- and with 50% into $\mu^+\mu^-$. For the background modes containing an J/ψ 200000 events have been generated each. The $\overline{\mathrm{p}}\mathrm{p} \to \pi^+\pi^-\eta$ and $\overline{\mathrm{p}}\mathrm{p} \to \pi^+\pi^-\pi^0$ decay modes need a much larger amount of events to show the needed suppression can be achieved. 10^7 or more events have been generated for these modes each. To save time, for these modes a generator-level filter is applied, which limits the invariant mass of the $\pi^+\pi^-$ under electron mass hypothesis to the J/ψ signal region $[2.8; 3.2]$ GeV/c^2 (see Appendix A). The corresponding filter efficiencies are listed in Tab. 5.

Reaction $\overline{\mathrm{p}}\mathrm{p} \to$	events	Filter eff. [%]	$p_{\bar{p}}$ [GeV/c]
$J/\psi\eta$	$4 \cdot 10^4$	100	6.003
$J/\psi\pi^0\pi^0$	$2 \cdot 10^5$	100	6.003
$J/\psi\pi^0\gamma$	$2 \cdot 10^5$	100	6.003
$J/\psi\eta\gamma$	$2 \cdot 10^5$	100	6.003
$J/\psi\eta$	$4 \cdot 10^4$	100	6.2316
$J/\psi\pi^0\pi^0$	$2 \cdot 10^5$	100	6.2316
$J/\psi\pi^0\gamma$	$2 \cdot 10^5$	100	6.2316
$J/\psi\eta\gamma$	$2 \cdot 10^5$	100	6.2316
$J/\psi\eta$	$4 \cdot 10^4$	100	6.9884
$J/\psi\eta\pi^0$	$2 \cdot 10^5$	100	6.9884
$J/\psi\pi^0\pi^0$	$2 \cdot 10^5$	100	6.9884
$J/\psi\pi^0\gamma$	$2 \cdot 10^5$	100	6.9884
$J/\psi\eta\gamma$	$2 \cdot 10^5$	100	6.9884
$\pi^+\pi^-\pi^0$	$9 \cdot 10^6$	13.2	6.9884
$J/\psi\eta$	$8 \cdot 10^4$	100	8.6819
$J/\psi\eta\eta$	$2 \cdot 10^5$	100	8.6819
$J/\psi\eta\pi^0$	$2 \cdot 10^5$	100	8.6819
$J/\psi\pi^0\pi^0$	$2 \cdot 10^5$	100	8.6819
$J/\psi\pi^0\gamma$	$2 \cdot 10^5$	100	8.6819
$J/\psi\eta\gamma$	$2 \cdot 10^5$	100	8.6819
$\pi^+\pi^-\eta$	10^7	13.8	8.6819
$\pi^+\pi^-\pi^0\pi^0$	10^7	13.8	8.6819
$\pi^+\pi^-\pi^0$	$2 \cdot 10^7$	14.0	8.6819

Table 5: Number of generated events and filter efficiencies for the generator level filter applied on the high-statistic background modes in the $J/\psi\eta$ analysis. For events containing a J/ψ no filter is applied. The J/ψ decays into e^+e^- and $\mu^+\mu^-$ with an equal branching ratio of 50%.

4.3 General reconstruction and selection

A likelihood-based selection algorithm based on the track information provided by the detector components is used for particle identification.
The $J/\psi \to e^+e^-$ candidates are reconstructed as described above in section 2. Track selection criteria for electrons have been defined using a sample of 10^7 events of the background channel $\overline{\mathrm{p}}\mathrm{p} \to \pi\pi\eta$ at a beam momentum of 8.6819 GeV/c. One daughter candidate from a J/ψ decay must be identified as an electron with a likelihood $\mathcal{L} > 85\%$, the other one as an electron with $\mathcal{L} > 99\%$; in that case a suppression greater than 10^7 is achieved for $\pi\pi\eta$ events

Reaction $\overline{\mathrm{p}}\mathrm{p} \to$	Beam mom. [GeV/c]	σ	$\mathcal{B}$
$J/\psi\eta$	6.003	σ_s	$2.34\% \times \mathcal{B}(\eta_c(2S) \to J/\psi\eta)$
$J/\psi\pi^0\pi^0$	6.003	σ_b	5.78%
$J/\psi\pi^0\gamma$	6.003	σ_b	5.84%
$J/\psi\eta\gamma$	6.003	σ_b	2.32%
$J/\psi\eta$	6.2316	σ_s	0.07%
$J/\psi\pi^0\pi^0$	6.2316	σ_b	5.78%
$J/\psi\pi^0\gamma$	6.2316	σ_b	5.84%
$J/\psi\eta\gamma$	6.2316	σ_b	2.32%
$J/\psi\eta$	6.9884	σ_s	$2.34\% \times \mathcal{B}(X(3872) \to J/\psi\eta)$
$J/\psi\eta\pi^0$	6.9884	σ_b	2.30%
$J/\psi\pi^0\pi^0$	6.9884	σ_b	5.78%
$J/\psi\pi^0\gamma$	6.9884	σ_b	5.84%
$J/\psi\eta\gamma$	6.9884	σ_b	2.32%
$\pi^+\pi^-\pi^0$	6.9884	$290\,\mu b$	98.80%
$J/\psi\eta$	8.6819	σ_s	$2.34\% \times \mathcal{B}(Y(4260) \to J/\psi\eta)$
$J/\psi\eta\eta$	8.6819	σ_b	0.92%
$J/\psi\eta\pi^0$	8.6819	σ_b	2.30%
$J/\psi\pi^0\pi^0$	8.6819	σ_b	5.78%
$J/\psi\pi^0\gamma$	8.6819	σ_b	5.84%
$J/\psi\eta\gamma$	8.6819	σ_b	2.32%
$\pi^+\pi^-\eta$	8.6819	$1.54\,\mu b$[1]	39.38%
$\pi^+\pi^-\pi^0\pi^0$	8.6819	$50\,\mu b$	97.61%
$\pi^+\pi^-\pi^0$	8.6819	$30 \pm 10\,\mu b$[2]	98.80%

Table 6: Cross sections and branching fractions for the $J/\psi\eta$ signal and background modes. For the J/ψ we use to the sole braching franction to one lepton type (the value for the braching fractions $\to e^+e^-$ and $\to \mu^+\mu^-$ are the same). σ_s denotes the cross section for the formation of a given resonance in $\overline{\mathrm{p}}\mathrm{p}$ events, $\mathcal{B}$ the branching fraction for the decay tree. σ_b is the cross section for the background mode in $\overline{\mathrm{p}}\mathrm{p}$ annihilation. 1) obtained from DPM generator. 2) measured value at 8.8GeV/c.

falsely identified as $J/\psi\eta$ (see App. A). The decay $J/\psi \to \mu^+\mu^-$ is also examined separately. Even with the highest PID criterium applied (*very tight*, muon identification likelihood $\mathcal{L} > 85\%$) still pions falsely identified as muons contribute to the $J/\psi\eta$ signal region.
The η candidates are reconstructed via $\eta \to \gamma\gamma$. Both identified γs are combined to an η candidate with an invariant mass in the intervall [0.47 : 0.62] GeV/c^2.
All $J/\psi\eta$ combinations found in an event are kinematically fitted by constraining the sum of the four-vector of the final state particles to the inital beam energy and momentum and constraining the origin of the charged final state particles to originate from a common vertex. A mass constraint is additionally applied on the η and J/ψ candidates (MB). The fit is repeated with mass constraints only (M) and with beam/energy constraints only (BC).
For accepted candidates the η mass (BC) is required to be in the region [0.535 : 0.565] GeV/c^2 and the J/ψ mass (BC) to be within [3.07 : 3.12] GeV/c^2. The confidence level of the fit with all constraints (MB) must be larger than 0.1%. If more than one candidate in an event passes these selection criteria, the candidate with the highest confidence level is chosen and the others are rejected. Reconstructed $J/\psi\eta$ candidates from the signal mode which are accepted by the criteria summarized above are checked if they are the correct combination. The resulting $J/\psi\eta$ invariant mass distributions for the four signal modes are shown in Fig. 7. In Tab. 7, the corresponding signal lineshape parameters are listed.
The background channels are reconstructed in the same way and pass the same selection criteria as the signal modes, without an check for the right combination.

4.4 Results

The reconstruction efficiency and the signal to noise ratios are examined separately for decays of $J/\psi \to e^+e^-$ and $\mu^+\mu^-$.

***J/ψη* at 6.0030 GeV/*c* [$\eta_c(2S)$]** The $J/\psi\eta$ signal region for this mode covers the interval [3.6447 : 3.6451] GeV/c^2 (Fig. 7a). At this beam momentum one is near the $J/\psi\eta$ phase space boundary, resulting in the shape of the distribution shown. The efficiency, calculated from the number of reconstructed candidates found in the $J/\psi\eta$ signal region after applying all selection criteria, is 15.7% for $J/\psi \to e^+e^-$ and 14.5% for $J/\psi \to \mu^+\mu^-$. The suppression for background modes is calculated from the ratio of the numbers of generated events and reconstructed $J/\psi\eta$ candidates in the signal region, the signal to noise ratio is calculated as described in section 3.4. A suppression of $> 10^5$ is obtained for $J/\psi\pi^0\pi^0$ and $J/\psi\pi^0\gamma$ for each J/ψ decay mode. The mode $J/\psi\eta\gamma$ yields to a high contamination of the signal region due to the missing low energy photon, with a suppression of only ≈ 5.

***J/ψη* at 6.2316 GeV/*c* [$\psi(2S)$]** For the $J/\psi\eta$ signal region we use the interval [3.68 : 3.693] GeV/c^2 (Fig. 7b). The reconstruction efficiency is 18.8% ($J/\psi \to e^+e^-$) and 17.7% ($J/\psi \to \mu^+\mu^-$). For the background mode $J/\psi\pi^0\pi^0$ a suppression $> 10^5$ for each J/ψ mode is obtained, while events are suppressed by a factor of 12500 resp. 33300 for $J/\psi\pi^0\gamma$ and in the order of 400 resp. 500 for $J/\psi\eta\gamma$.

***J/ψη* at 6.9884 GeV/*c* [$X(3872)$]** The $J/\psi\eta$ signal region is defined as the interval [3.86 : 3.885] GeV/c^2. We have a reconstruction efficiency of 18.6% and 16.9% for $J/\psi \to e^+e^-$ and $J/\psi \to \mu^+\mu^-$, respectively. The background modes $J/\psi\eta\pi^0$ and $J/\psi\pi^0\pi^0$ are suppressed by a factor $> 10^5$ for each J/ψ mode. The suppression for $J/\psi\pi^0\gamma$ is 8300 resp. 16700, and about 2000 resp. 1800 for $J/\psi\eta\gamma$. The analysis of the background mode $\overline{\mathrm{p}}\mathrm{p} \to \pi^+\pi^-\pi^0$ at this beam momentum, with a generator-level efficiency of 13.2%, leads to a suppression of $7 \cdot 10^7$. This corresponds to a signal-to-noise ratio of $S/N = 1\tilde{\sigma}/nb$, where the unknown values are expressed by $\tilde{\sigma} = \sigma_s(\overline{\mathrm{p}}\mathrm{p} \to X) \times \mathcal{B}(X \to J/\psi\eta)$.

***J/ψη* at 8.6819 GeV/*c* [$Y(4260)$]** The $J/\psi\eta$ signal region for this mode covers the interval [4.22 : 4.3] GeV/c^2. The reconstruction efficiencies are 18.8% and 16.8% for $J/\psi \to e^+e^-$ resp. $J/\psi \to \mu^+\mu^-$. The background modes $J/\psi\eta\eta$, $J/\psi\eta\pi^0$ and $J/\psi\pi^0\pi^0$ are suppressed by $> 10^5$ for each J/ψ mode. $J/\psi\pi^0\gamma$ is suppressed by 3600 resp. 5300 and $J/\psi\eta\gamma$ by 3400 resp. 3700. The background mode $\overline{\mathrm{p}}\mathrm{p} \to \pi^+\pi^-\eta$ has been produced with a generator level filter applied, which has an efficiency of 13.8%. The suppression achieved is $> 7 \cdot 10^7$ for the mode $J/\psi \to e^+e^-$. In the case of $J/\psi \to \mu^+\mu^-$ only a suppression of 59000 is possible. The expected signal to noise ratio S/N is thus $369\tilde{\sigma}$/nb resp. $0.3\tilde{\sigma}$/nb. The analysis of the background mode $\overline{\mathrm{p}}\mathrm{p} \to \pi^+\pi^-\pi^0$ at this energy, with a generator-level efficiency of 14.0%, leads to a suppression of $1.4 \cdot 10^8$ each, yielding $S/N = 15\tilde{\sigma}$/nb resp. $17\tilde{\sigma}$/nb.

Decay into $J/\psi\eta$	Mean [GeV/c^2]	FWHM [GeV/c^2]	J/ψ mean [GeV/c^2]
$\eta_c(2S)$	3.645	0.001	3.093
$\psi(2S)$	3.686	0.005	3.094
$X(3872)$	3.872	0.011	3.096
$Y(4260)$	4.260	0.018	3.096

Table 7: Signal parameters. Listed are the mean and width (FWHM) of the $J/\psi\eta$ signal and the mean of the J/ψ signal.

Decay into $J/\psi\eta$	beam mom. [GeV/c]	efficiency [%]	
		ϵ_{s,e^+e^-}	$\epsilon_{s,\mu^+\mu^-}$
$\eta_c(2S)$	6.0030	15.7	14.5
$\psi(2S)$	6.2316	18.8	17.7
$X(3872)$	6.9884	18.6	16.9
$Y(4260)$	8.6819	18.8	16.8

Table 8: Reconstruction efficiency ϵ_s for the four $J/\psi\eta$ signal modes. The J/ψ decays to e^+e^- and $\mu^+\mu^-$ are examined separately.

The expected number of events per day is listed in Tab. 10, using the formula $N = \epsilon_s\tilde{\sigma}\int\mathcal{L}dt$, with $\mathcal{L} = 2\cdot10^{32}\text{cm}^{-2}\text{s}^{-1}$

5 Study of the $\psi(2S)\pi^+\pi^-$ system

The $Y(4320)$ has been observed by BaBar in 2007. Its mass is stated as 4324 ± 24 MeV/c^2, the width as 172 ± 33 MeV/c^2. In this section the formation of the $Y(4320)$ in $\overline{\text{p}}\text{p}$ annihilation is studied at a beam momentum of $p_{\bar{p}} = 8.9578$ GeV/c. The resonance is reconstructed from its decay into $\psi(2S)\pi^+\pi^-$, with $\psi(2S) \to J/\psi\pi^+\pi^-$ and $J/\psi \to l^+l^-$.

Decay	Exp. number of events/day	
	$N_{e^+e^-}$	$N_{\mu^+\mu^-}$
$\eta_c(2S) \to J/\psi\eta$	$63\tilde{\sigma}\text{nb}^{-1}$	$58\tilde{\sigma}\text{nb}^{-1}$
$\psi(2S) \to J/\psi\eta$	$75\tilde{\sigma}\text{nb}^{-1}$	$71\tilde{\sigma}\text{nb}^{-1}$
$X(3872) \to J/\psi\eta$	$75\tilde{\sigma}\text{nb}^{-1}$	$68\tilde{\sigma}\text{nb}^{-1}$
$Y(4260) \to J/\psi\eta$	$76\tilde{\sigma}\text{nb}^{-1}$	$67\tilde{\sigma}\text{nb}^{-1}$

Table 10: Expected number of events per day under design luminosity, given in units of the unknown cross section $\tilde{\sigma}$ for the $J/\psi\eta$ analysis.

5.1 Background considerations

The dominant background mode is

- $\overline{\text{p}}\text{p} \to \pi^+\pi^-\pi^+\pi^-\pi^+\pi^-$

5.2 Data samples

40000 events of the signal mode $\overline{\text{p}}\text{p} \to \psi(2S)\pi^+\pi^-, \psi(2S) \to J/\psi\pi^+\pi^-$ have been generated, with a branching fraction of 50% each for $J/\psi \to e^+e^-$ and $J/\psi \to \mu^+\mu^-$.
For the background mode 10^6 events of the reaction $\overline{\text{p}}\text{p} \to 3\pi^+3\pi^-$ have been generated. A generator-level filter is applied, which requires the invariant mass of at least one $\pi^+\pi^-$ combination (under electron mass hypothesis) to be within the J/ψ signal region $[2.8; 3.2]$ GeV/c^2 (see Appendix A). The filter efficiency for this mode is 0.67%.

5.3 General reconstruction and selection

A likelihood-based selection algorithm based on the track information provided by the detector components is used for particle identification.
The $J/\psi \to e^+e^-$ candidates are reconstructed as described in section 2. Both daughter candidates from a J/ψ decay must be identified as electrons, one with a likelihood of $\mathcal{L} > 85\%$ and one $\mathcal{L} > 99$. The decay $J/\psi \to \mu^+\mu^-$ is separately examined, requring for muon identification a likelihood $\mathcal{L} > 85\%$. The likelihood value for the particle candidates identified as pions must be $\mathcal{L} > 0.2$. J/ψ candidates are then combined with two oppositely charged pions to $\psi(2S)$ candidates. Finally these are combined with another two oppositely charged pions.
All $J/\psi\pi^+\pi^-\pi^+\pi^-$ combinations found in an event are kinematically fitted by constraining the sum of the four-vector of the final state particles to the inital beam energy and momentum and constraining the origin of the charged final state particles to originate from a common vertex. Also a mass constraint is applied on the J/ψ and $\psi(2S)$ candidates (MB). The fit is repeated with mass constraints only (M) and with beam/energy constraints only (BC).
For accepted candidates the $\psi(2S)$ (BC) is required to be within the interval $[3.67 : 3.71]$ GeV/c^2 and the J/ψ mass (BC) to be within $[3.07 : 3.12]$ GeV/c^2. The confidence level of the fit (MB) must be larger than 0.1%. If more than one candidate in an event passes these selection criteria, the candidate with the highest confidence level is chosen and the others are rejected. Reconstructed $\psi(2S)\pi\pi$ candidates

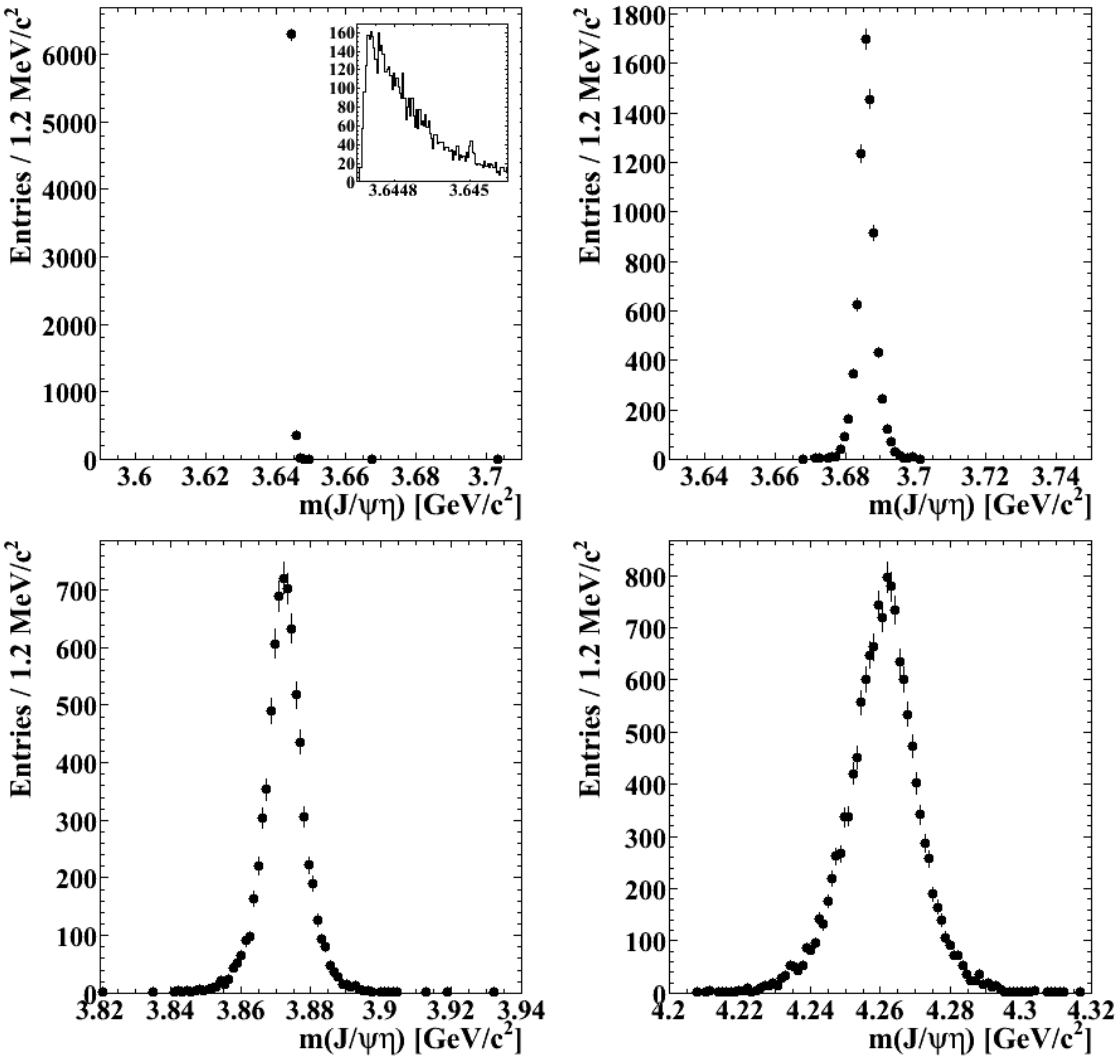

Figure 7: Invariant mass distribution for $J/\psi\eta$ candidates for different beam momenta. a) $p_{\bar{p}} = 6.0030$ GeV/c; b) $p_{\bar{p}} = 6.2316$ GeV/c; c) $p_{\bar{p}} = 6.9884$ GeV/c; d) $p_{\bar{p}} = 8.6819$ GeV/c. The insert in a) shows a close-up of the narrow signal region.

Decay	beam mom.	suppression		Signal to noise	
$\overline{\mathrm{p}}\mathrm{p} \to$	[GeV/c]	$\eta_{e^+e^-}$	$\eta_{\mu^+\mu^-}$	$S/N_{e^+e^-}$	$S/N_{\mu^+\mu^-}$
$J/\psi\pi^0\pi^0$	6.0030	$> 10^5$	$> 10^5$	$6300\tilde{\sigma}/\sigma_b$	$5800\tilde{\sigma}/\sigma_b$
$J/\psi\pi^0\gamma$	6.0030	$> 10^5$	$> 10^5$	$6200\tilde{\sigma}/\sigma_b$	$5700\tilde{\sigma}/\sigma_b$
$J/\psi\eta\gamma$	6.0030	5	6	$1\tilde{\sigma}/\sigma_b$	$1\tilde{\sigma}/\sigma_b$
$J/\psi\pi^0\pi^0$	6.2316	$> 10^5$	$> 10^5$	$7600\tilde{\sigma}/\sigma_b$	$7100\tilde{\sigma}/\sigma_b$
$J/\psi\pi^0\gamma$	6.2316	12500	33300	$900\tilde{\sigma}/\sigma_b$	$2300\tilde{\sigma}/\sigma_b$
$J/\psi\eta\gamma$	6.2316	400	500	$100\tilde{\sigma}/\sigma_b$	$100\tilde{\sigma}/\sigma_b$
$J/\psi\eta\pi^0$	6.9884	$> 10^5$	$> 10^5$	$18800\tilde{\sigma}/\sigma_b$	$17100\tilde{\sigma}/\sigma_b$
$J/\psi\pi^0\pi^0$	6.9884	$> 10^5$	$> 10^5$	$75\tilde{\sigma}/\sigma_b$	$6800\tilde{\sigma}/\sigma_b$
$J/\psi\pi^0\gamma$	6.9884	8300	16700	$600\tilde{\sigma}/\sigma_b$	$1100\tilde{\sigma}/\sigma_b$
$J/\psi\eta\gamma$	6.9884	2000	1800	$400\tilde{\sigma}/\sigma_b$	$300\tilde{\sigma}/\sigma_b$
$\pi^+\pi^-\pi^0$	6.9884	$> 7 \cdot 10^7$	$> 7 \cdot 10^7$	$1\tilde{\sigma}/\mathrm{nb}$	$1\tilde{\sigma}/\mathrm{nb}$
$J/\psi\eta\eta$	8.6819	$> 10^5$	$> 10^5$	$47700\tilde{\sigma}/\sigma_b$	$42600\tilde{\sigma}/\sigma_b$
$J/\psi\eta\pi^0$	8.6819	$> 10^5$	$> 10^5$	$19000\tilde{\sigma}/\sigma_b$	$17000\tilde{\sigma}/\sigma_b$
$J/\psi\pi^0\pi^0$	8.6819	$> 10^5$	$> 10^5$	$7600\tilde{\sigma}/\sigma_b$	$6800\tilde{\sigma}/\sigma_b$
$J/\psi\pi^0\gamma$	8.6819	3600	5300	$300\tilde{\sigma}/\sigma_b$	$400\tilde{\sigma}/\sigma_b$
$J/\psi\eta\gamma$	8.6819	3400	3700	$600\tilde{\sigma}/\sigma_b$	$600\tilde{\sigma}/\sigma_b$
$\pi^+\pi^-\eta$	8.6819	$> 7 \cdot 10^7$	$6 \cdot 10^4$	$500\tilde{\sigma}/\mathrm{nb}$	$0.4\tilde{\sigma}/\mathrm{nb}$
$\pi^+\pi^-\pi^0$	8.6819	$> 1.4 \cdot 10^8$	$> 1.4 \cdot 10^8$	$20\tilde{\sigma}/\mathrm{nb}$	$18\tilde{\sigma}/\mathrm{nb}$
$\pi^+\pi^-\pi^0\pi^0$	8.6819	$> 1.7 \cdot 10^8$	$1.7 \cdot 10^8$	$15\tilde{\sigma}/\mathrm{nb}$	$14\tilde{\sigma}/\mathrm{nb}$

Table 9: Suppression η and signal to noise ratio for the background modes of the $J/\psi\eta$ analysis, which are separately examined for the decay modes $J/\psi \to e^+e^-$ and $J/\psi \to \mu^+\mu^-$. The signal to noise ratios are given in terms of the unknown cross section $\tilde{\sigma}$ or $\tilde{\sigma}/\sigma_b$.

from the signal mode which are accepted by the criteria summarized above are checked if they are the correct combination.
The background channels are reconstructed in the same way and pass the same selection criteria as the signal modes, without an check for the right combination.

5.4 Results

The reconstruction efficiency and the signal to noise ratio are examined separately for decays of $J/\psi \to e^+e^-$ and $\mu^+\mu^-$.
The $\psi(2S)\pi\pi$ signal region is defined as the interval from [4.29 : 4.35] GeV/c^2. The reconstruction efficiency is 14.9% ($J/\psi \to e^+e^-$) and 12.2% ($J/\psi \to \mu^+\mu^-$). The reconstructed signal has a mean of 4320 MeV/c^2 and a width (FWHM) of 13 MeV/c^2.
The cross section for the background mode $\overline{\mathrm{p}}\mathrm{p} \to 3\pi^+3\pi^-$ is 140 μb (measured at a beam momentum of 8.8 GeV/c). Suppression and signal to noise ratio are examined separately for $J/\psi \to e^+e^-$ and $J/\psi \to \mu^+\mu^-$. The suppression for this mode is $\eta_{e^+e^-} = 37 \cdot 10^6$ and $\eta_{\mu^+\mu^-} = 25 \cdot 10^6$. The signal to noise ratios are thus $S/N_{ee} = 700\tilde{\sigma}/\,\mu\mathrm{b}$ and $S/N_{\mu^+\mu^-} = 400\tilde{\sigma}/\,\mu\mathrm{b}$, where $\tilde{\sigma} = \sigma_S(\overline{\mathrm{p}}\mathrm{p} \to Y(4320))\mathcal{B}(Y(4320) \to \psi(2S)\pi^+\pi^-)$ is given in terms of the unknown signal cross section and branching fraction.

Reaction	Beam mom.	events	Filter eff.
$\overline{\mathrm{p}}\mathrm{p} \to$	[GeV/c]		[%]
$\psi(2S)\pi^+\pi^-$	8.9578	20000	100
$3\pi^+3\pi^-$	8.9578	10^6	0.67

Table 11: Signal and background modes for the $\psi(2S)\pi^+\pi^-$ analysis.

6 Charmonium Hybrid in the $\chi_{c1}\pi^0\pi^0$ Decay Mode

The charmonium hybrid ground state is generally expected to be a spin-exotic $J^{PC} = 1^{-+}$ state and lattice QCD calculations predict its mass in the range between 4100 and 4400 MeV/c^2 [**?**, **?**, **?**]. In $\overline{\mathrm{p}}\mathrm{p}$ annihilation this state can be produced only in association with one or more recoiling particles. Here the results of a study assuming the production of a state having a mass 4290 MeV/c^2 and a width of 20 MeV together with a η meson in $\overline{\mathrm{p}}\mathrm{p}$ annihilaton

Reaction $\overline{\mathrm{p}}\mathrm{p} \to$	σ	$\mathcal{B}$
$\psi(2S)\pi^+\pi^-$	$\sigma_s(\overline{\mathrm{p}}\mathrm{p} \to Y(4320))$	$1.9\% \times \mathcal{B}(Y(4320) \to \psi(2S)\pi^+\pi^-)$
$3\pi^+3\pi^-$	140 μb	100%

Table 12: Cross sections and branching fractions for the $J/\psi\eta$ signal and background modes. For the subsequent J/ψ decay we use to the sole braching franction to one lepton type (the value for the braching fractions $\to e^+e^-$ and $\to \mu^+\mu^-$ are the same). The cross section for the background mode has been measured at a beam momentum of 8.8 GeV/c.

Decay	efficiency		suppression		Signal to noise	
$\overline{\mathrm{p}}\mathrm{p} \to$	ϵ_{S,e^+e^-}	$\epsilon_{S,\mu^+\mu^-}$	$\eta_{e^+e^-}$	$\eta_{\mu^+\mu^-}$	$S/N_{e^+e^-}$	$S/N_{\mu^+\mu^-}$
$\psi(2S)\pi^+\pi^-$	14.9%	12.2%	–	–		
$3\pi^+3\pi^-$	–	–	$37 \cdot 10^6$	$25 \cdot 10^6$	$700\tilde{\sigma}$	$400\tilde{\sigma}$

Table 13: Suppression η and signal to noise ratio for the background modes of the $J/\psi\eta$ analysis, which are separately examined for the decay modes $J/\psi \to e^+e^-$ and $J/\psi \to \mu^+\mu^-$. The signal to noise ratios are given in terms of the unknown cross section $\tilde{\sigma}$.

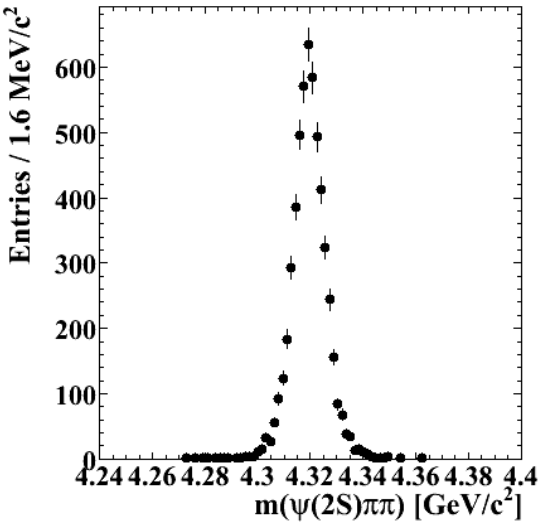

Figure 8: Invariant mass distribution for $\psi(2S)\pi\pi$ candidates.

at $\sqrt{s} = 5.473$GeV are reported.

Flux-tube model calculations predict for a hybrid state of this mass suppressed decays to open charm with respect to hidden charm decays [**?**]. An OZI-allowed decay to hidden charm would be the transition to χ_{c1} with emission of light hadrons, preferable scalar particles [**?**]. The lightest scalar system is composed out of two neutral pions in a relative s-wave.

In the study the decay of the charmonium hybrid (labeled as ψ_g in the following) to $\chi_{c1}\,\pi^0\,\pi^0$ with the subsequent radiative $\chi_{c1} \to J/\psi\,\gamma$ decay with J/ψ decaying to a lepton pair e^+e^- and $\mu^+\mu^-$ is considered. The recoiling meson is reconstructed from the decay $\eta \to \gamma\,\gamma$.

6.1 Signal cross section

For the production of ψ_g in $\overline{\mathrm{p}}\mathrm{p} \to \psi_g\eta$ it is assumed that the cross section is in the same order of magnitude as for the process $\overline{\mathrm{p}}\mathrm{p} \to \psi(2S)\eta$ including conventional charmonium. The cross section for this reaction is given in Ref. [**?**] to be (33 ± 8) pb at $\sqrt{s} = 5.38$GeV and is calculated from the crossed process $\psi(2S) \to \eta\overline{\mathrm{p}}\mathrm{p}$ observed in e^+e^- annihilation.

6.2 Background Considerations

The final state with 7 photons and an e^+e^- lepton pair originating from J/ψ decays has a distinctive signature and separation from light hadron back-

Reaction $\overline{\mathrm{p}}\mathrm{p} \to$	σ	$\mathcal{B}$
$\psi_g\eta$	33 pb	$1.63\% \times \mathcal{B}(\psi_g \to \chi_{c1}\pi^0\pi^0)$
$\chi_{c0}\pi^0\pi^0\eta$	?	0.059%
$\chi_{c1}\pi^0\eta\eta$	?	0.648%
$\chi_{c1}\pi^0\pi^0\pi^0\eta$	?	1.61%
$J/\psi\pi^0\pi^0\pi^0\eta$	?	4.51%

Table 14: Cross sections for signal and background reactions. The table lists also the product of branching fractions for the subsequent particle decays.

Reaction $\overline{\mathrm{p}}\mathrm{p} \to$	Events
$\psi_g\eta$	$2 \cdot 10^5$
$\chi_{c0}\pi^0\pi^0\eta$	$2 \cdot 10^5$
$\chi_{c1}\pi^0\eta\eta$	$2 \cdot 10^5$
$\chi_{c1}\pi^0\pi^0\pi^0\eta$	$2 \cdot 10^5$
$J/\psi\pi^0\pi^0\pi^0\eta$	$2 \cdot 10^5$

Table 15: Nubmer of analyzed signal and background events. The J/ψ decays with equal branching fraction of 50% into e^+e^- and $\mu^+\mu^-$.

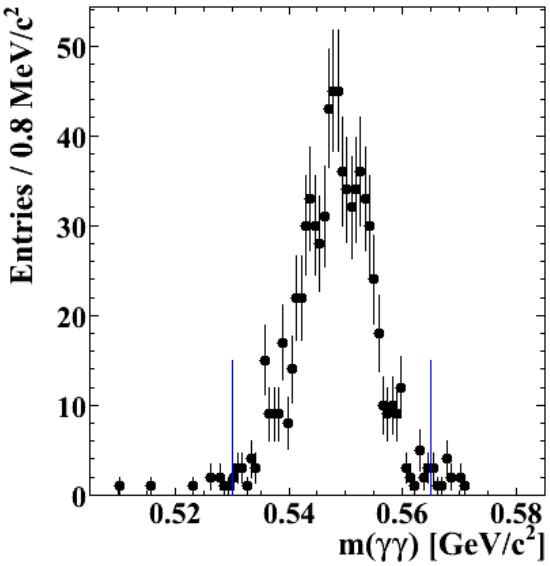

Figure 9: Invariant $\eta \to \gamma\gamma$ mass obtained after the kinematic fit with a momentum and energy constraint on the initial $\overline{\mathrm{p}}\mathrm{p}$ system as described in the text.

ground should be feasible. Another source of background are events with hidden charm, in particular events including a J/ψ meson. This type of background has been studied by analyzing $\overline{\mathrm{p}}\mathrm{p} \to \chi_{c0}\,\pi^0\,\pi^0\,\eta$, $\overline{\mathrm{p}}\mathrm{p} \to \chi_{c1}\,\pi^0\,\eta\,\eta$, $\overline{\mathrm{p}}\mathrm{p} \to \chi_{c1}\,\pi^0\,\pi^0\,\pi^0\,\eta$ and $\overline{\mathrm{p}}\mathrm{p} \to J/\psi\,\pi^0\,\pi^0\,\pi^0\,\eta$. The hypothetical hybrid state is absent in these reactions, but the χ_{c0} and χ_{c1} mesons decay via the same decay path as for signal. Therefore these events have a similar topology as signal events and could potentially pollute the ψ_g signal.

6.3 Data Sample

The number of analyzed signal and background events is summarized in Table 15.

6.4 Reconstruction

Photon candidates are selected from the clusters found in the EMC with the reconstruction algorithm explained in Sec. **??**. Two photon candidates are combined and accepted as π^0 and η candidates if their invariant mass is within the interval $[115;150]\,\mathrm{MeV}/c^2$ and $[470;610]\,\mathrm{MeV}/c^2$, respectively.

From the J/ψ and photon candidates found in an event $\chi_{c1} \to J/\psi\,\gamma$ candidates are formed, whose invariant mass is within the range $[3.3;3.7]\mathrm{GeV}/c^2$. From these $\chi_{c1}\,\pi^0\,\pi^0\,\eta$ candidates are created, where the same photon candidate does not occur more than once in the final state. The corresponding tracks and photon candidates of the final state are kinematically fitted by constraining their momentum and energy sum to the initial $\overline{\mathrm{p}}\mathrm{p}$ system and the invariant lepton candidates mass to the J/ψ mass. Accepted candidates must have a confidence level of $CL > 0.1\%$ and the invariant mass of the $J/\psi\,\gamma$ subsystem should be within the range $[3.49; 3.53]\,\mathrm{GeV}/c^2$, whereas the invariant mass of the η candidates must be within the interval $[530; 565]\,\mathrm{MeV}/c^2$. A FWHM of $13\mathrm{MeV}/c^2$ and $9\mathrm{MeV}/c^2$ is observed for the η and χ_{c1} signal respectively (Figs. **??**) after the kinematic fit.

For the final event selection the same kinematic fit is repeated with additionally constraining the invariant χ_{c1}, π^0 and η mass to the corresponding nominal mass values. Candidates having a confidence level less than 0.1% are rejected.

In XXX% of the events more than one accepted candidate is found and the candidate having the highest confidence level of the final event fit is chosen. In XXX% of the cases the correct candidate is accepted. In only XXX% of all events an event reconstructed in the wrong combination is falsely accepted. Thus the signal pollution with these events is neglegible. To estimate the reconstruction efficiency only the correct combinations are considered.

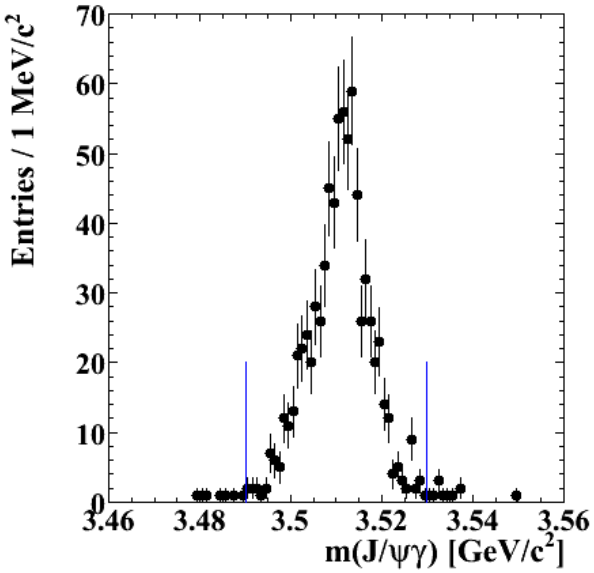

Figure 10: Invariant $\chi_{c1} \to J/\psi\gamma$ mass obtained after the kinematic fit with a momentum and energy constraint on the initial $\overline{\mathrm{p}}\mathrm{p}$ system as described in the text. The J/ψ is reconstructed from the e^+e^- decay mode.

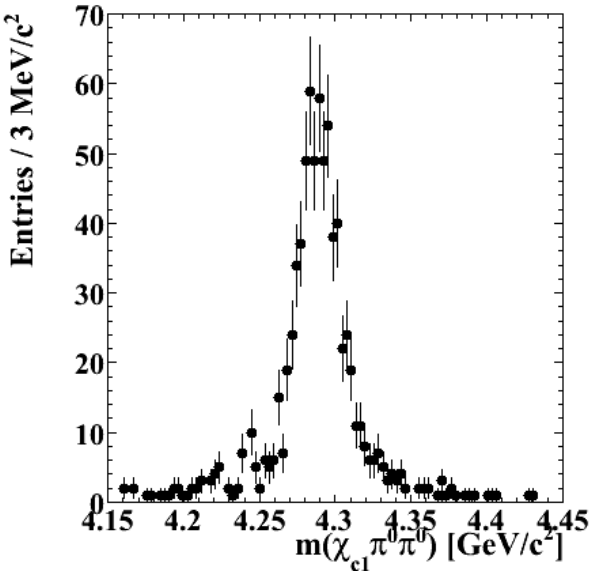

Figure 11: Invariant $\chi_{c1}\pi^0\pi^0$ mass obtained for the $J/\psi \to e^+e^-$ channel after application of all selection criteria.

6.5 Results

The invariant $\chi_{c1}\pi^0\pi^0$ mass obtained after application of all selection criteria is shown in Fig. **??**. The ψ_g signal has a FWHM of 30MeV/c^2. The reconstruction efficiency is determined from the number of ψ_g signal entries in the mass range $4.24 - 4.33$GeV/c^2. The reconstruction efficiency is found to be 2.71% ($J/\psi \to e^+e^-$) and 2.42% ($J/\psi \to \mu^+\mu^-$).

The background suppression is estimated from the number of accepted background events after application of all selection criteria having a valid ψ_g candidate whose invariant mass is within the same intervall used to determine the reconstruction efficiency for signal events. In Table 16 the yielded suppression for the individual background channels is listed together with the expected signal to background ratio S/N, which is reported in terms of

$$\mathcal{R} = \frac{\sigma_S \mathcal{B}(\psi_g \to \chi_{c1}\pi^0\pi^0)}{\sigma_B} \qquad (3)$$

given by the unknown signal (background) cross section σ_S (σ_B) and the branching fraction for the $\psi_g \to \chi_{c1}\pi^0\pi^0$ decay. Depending on the background channel and reconstructed J/ψ decay mode S/N is varying between $610 - 3200\,\mathcal{R}$. For $\overline{\mathrm{p}}\mathrm{p} \to \chi_{c1}\pi^0\pi^0\pi^0\eta$ only a lower limit $> 2700\,\mathcal{R}$ ($J/\psi \to e^+e^-$) and $> 2500\,\mathcal{R}$ ($J/\psi \to \mu^+\mu^-$) is obtained. If the cross sections σ_B for the background processes are not enhanced by more than an order of magnitude over $\sigma_S\mathcal{B}(\psi_g \to \chi_{c1}\pi^0\pi^0)$ very low contamination of the signal from these processes is expected.

Background reactions including no charm but light mesons in the final state have not been investigated yet. The studies of these background types performed for the charmonium states presented in this document proof that a clean reconstruction via the $J/\psi \to e^+e^-$ decay mode is possible. Therefore the reconstruction of the ψ_g state via this decay should yield also a sufficient background suppression. Since the results of the other studies showed also that the reconstruction via $J/\psi \to \mu^+\mu^-$ is presently not feasible the analyis is restricted to the $J/\psi \to e^+e^-$ decay mode only. Then the expected number of reconstructed events per day is given by

$$N = \sigma_S \mathcal{B}(\psi_g \to \chi_{c1}\pi^0\pi^0) \times 7.5\,\mathrm{nb}^{-1} \qquad (4)$$

As afore said the cross section for $\overline{\mathrm{p}}\mathrm{p} \to \psi(2S)\eta$ is expected to be 33 pb. Assuming the same cross section for the production of the charmonium hybrid state this becomes $N = 0.25\mathcal{B}(\psi_g \to \chi_{c1}\pi^0\pi^0)$ events per day.

7 Charmonium Hybrid in $D^0\overline{D}^{*0}$ Decay Mode

The selection of π^0 and η candidates is the same as described in Sec. **??**. Pions and kaons are selected from charged particles in the event by apply-

Reaction $\overline{\mathrm{p}}\mathrm{p} \to$	$\eta_{e^+e^-}$ $[10^3]$	$\eta_{\mu^+\mu^-}$ $[10^3]$	$S/N_{e^+e^-}$ $[10^3]$	$S/N_{\mu^+\mu^-}$ $[10^3]$
$\chi_{c0}\pi^0\pi^0\eta$	4.3	3	$3.2\,\mathcal{R}$	$2\,\mathcal{R}$
$\chi_{c1}\pi^0\eta\eta$	20	10	$1.4\,\mathcal{R}$	$0.61\,\mathcal{R}$
$\chi_{c1}\pi^0\pi^0\pi^0\eta$	> 100	> 100	$> 2.7\,\mathcal{R}$	$> 2.5\,\mathcal{R}$
$J/\psi\pi^0\pi^0\pi^0\eta$	91	38	$0.89\,\mathcal{R}$	$0.33\,\mathcal{R}$

Table 16: Background suppression η and the ψ_g signal to background ratio S/N for the individual background reactions. $\mathcal{R}$ is the ratio of the signal cross section

ing a likelihood based selection algorithm, where a likelihood value of $\mathcal{L} > 0.2$ is required to accept a candidate as a pion or kaon. All possible $K^+\pi^-\pi^0$ combinations having an invariant mass in the range $[1.7; 2.2]\mathrm{GeV}/c^2$ in an event are formed and fitted by applying a π^0 mass constraint and requiring a common vertex for the tracks of the two charged candidates. A confidence level $CL > 0.1\%$ is required to accept the candidates as $D^0 \to K^+\pi^-\pi^0$ candidates. These are then used to form $D^0\pi^0$ candidates having an invarinat mass in the intervall $[1.95; 2.05]\mathrm{GeV}/c^2$, which are kinematically fitted applying a π^0 mass constraint. If the fit yields a confidence level $CL > 0.1\%$ the $D^{*0} \to D^0\pi^0$ candidate is accepted for further selection. Afterwards $D^0\overline{D}^{*0}\eta$ combinations are formed and fitted by constraining the final state particles' four-vectors to the inital $\overline{\mathrm{p}}\mathrm{p}$ system momentum and energy. Furtheron the invariant $\gamma\gamma$ mass of the π^0 candidates in the decay tree is constrained to the π^0 mass. A confidence level of $CL > 0.1\%$ is required.

For final event selection the fit is repeated but with additional mass constraints on the D^0, D^{*0} and η candidates. Candidates leading to a confidence level lower than 0.1% are discarded.

A candidate multiplicity higher than one is observed in XXX% of the reconstructed events. Only the candidate leading to the highest confidence level is accepted for further analysis. In XXX% of the cases the combination corresponding to the generated combination is selected. The pollution of the signal with falsely combined candidates is therefore less than XXX and negligible. To estimate the reconstruction efficiency only the correct combinations are considered. The event yield is determined as the number of $D^0\overline{D}^{*0}$ signal entries falling in the mass window $[4.24; 4.35]\mathrm{GeV}/c^2$.

7.1 Results

The obtained $D^0\overline{D}^{*0}$ invariant mass distribution is shown Fig. **??**. A signal width (FWHM) of XXXMeV/c^2 is observed. The reconstruction efficiency is 4.5%.

The background reactions $\overline{\mathrm{p}}\mathrm{p} \to D^0\overline{D}^{*0}\eta$ (with $D^0 \to K^+\pi^-\pi^0\pi^0$) and $\overline{\mathrm{p}}\mathrm{p} \to D^0\overline{D}^{*0}\pi^0$ could be suppressed by a factor $> 2 \cdot 10^5$. Assuming equal cross sections for these processes and signal events and a branching fraction for $D^0 \to K^+\pi^-\pi^0\pi^0$ (which is listed by the PDG as seen) in the order of 5% the expected signal to noise ratio can be expressed by

$$\frac{S}{N} > \frac{\mathcal{B}(\psi_g \to D^0\overline{D}^{*0}) \times 0.47\% \times 4.5\%}{(0.16\% + 1.17\%) \times 5 \cdot 10^{-6}} \quad (5)$$

$$= \mathcal{B}(\psi_g \to D^0\overline{D}^{*0}) \times 3.2 \cdot 10^3, \quad (6)$$

where the term $\mathcal{B}(\psi_g \to D^0\overline{D}^{*0})$ is the unknown branching fraction for the decay $\psi_g \to D^0\overline{D}^{*0}$.

With the assumed cross section of 30 pb and design luminosity $\mathcal{L} = 2 \cdot 10^{32}\mathrm{cm}^{-2}\mathrm{s}^{-1}$ the expected number of reconstructed events per day is given by

$$N = \mathcal{B}(\psi_g \to D^0\overline{D}^{*0}) \times 0.11. \quad (7)$$

If one defines the significance as $S/\sqrt{S+N}$ one yields with the assumptions made above the follwing formular

$$\frac{\sigma_S \epsilon \mathcal{B}_S \sqrt{\mathcal{L}t}}{\sqrt{(\sigma_S \epsilon \mathcal{B}_S + \sigma_B \eta \mathcal{B}_B)}}, \quad (8)$$

where σ_S and σ_B are the signal and background cross sections, $\mathcal{B}_S$ and $\mathcal{B}_B$ label the product of branching ratios for signal and background reactions and the time of data taking is given by t. The significance is shown in dependence of t in Fig. 12, where the above assumptions on the cross sections ($\sigma_S = \sigma_B$) and the branching fraction $\mathcal{B}(D^0 \to K^+\pi^-\pi^0\pi^0) = 5\%$ have been made. The branching fraction $\mathcal{B}(\psi_g \to D^0\overline{D}^{*0})$ has been set to 1, 0.30 and 0.13 Assuming that Panda will run half of its lifetime (corresponding to $\approx$ 850 days) at a beam momentum of 15GeV/c a significance

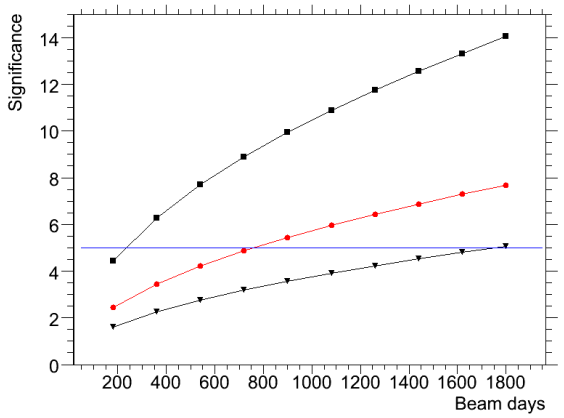

Figure 12: Expected significance for the reaction $\overline{\mathrm{p}}\mathrm{p} \to \psi_g\eta$ in dependence of the beam time. The significance is shown for three values of the branching fraction $\mathcal{B}(\psi_g \to D^0\overline{D}^{*0})$: 1 (black squares), 0.3 (red circles) and 0.13 (black triangles). The blue line marks a significance level of 5.

> 5 can be reached only if the branching fraction $\mathcal{B}(\psi_g \to D^0\overline{D}^{*0})$ is above 30%. This corrsesponds to a total of $\approx$ 30 reconstructed events. If the branching fraction is below 13% Panda will not be able to detect the ψ_g reconstructed from the studied decay mode with sufficent significance level within the entire lifetime. To be sensitive to lower branching fractions the D^0, D^{*0} and the recoil η mesons have to reconstructed from other decay modes and decays into $D^+\overline{D}^{*-}$ have to be taken into account also.

In conclusion this study proofs that the reconstruction of an object of a mass of $\approx$ 4GeV/c^2 decaying to open charm produced in $\overline{\mathrm{p}}\mathrm{p}$ annihilation at 15GeV/c with a recoiling η meson leading to a final state with high photon multiplicity is feasible. The low branching fractions of D mesons make the inclusion of other decay modes neccessary to be sensitive for lower ψ_g branching fractions, but these decays should be detectable with similar efficiency as the decay mode presented in this study.

A Generator filter method

A.1 Introduction

To achieve the relevant number of background events for benchmark channels including a J/ψ in a reasonable time, it has been decided to apply an event filter on the generator level. The strategy is to consider only events where the invariant mass of two charged particles (with the hypothesis that it was a e^+e^- pair) are within a certain J/ψ mass window.

$\mathcal{L}_{e^+e^-}$		No of reconstr. events		
$e^\pm$	$e^\mp$	SR	SB_l	SB_r
$> 0\%$	$> 0\%$	204269	0	0
$> 0\%$	$> 20\%$	18965		
$> 20\%$	$> 20\%$	338		
$> 20\%$	$> 85\%$	64		
$> 85\%$	$> 85\%$	3		
$> 85\%$	$> 99\%$	1		
$> 99\%$	$> 99\%$	0		

Table 17: Number of reconstructed $J/\psi\eta$ candidates from the background mode $\pi\pi\eta$, for three regions of the generated invariant $\pi\pi$ mass under electron mass hypothesis: J/ψ signal region SR and left and right J/ψ sidebanmd regions (SB_l and SB_r, resp.).

A.2 Validation of the generator filter method on the $J/\psi\eta$ analysis

In this analysis one relevant background channel is $\pi\pi\eta$. It had to be justified that the generated mass of the $\pi\pi$ system, with the pions falsely identified as electrons, can be limited to the J/ψ signal region.
A generator-level filter is applied in the following way. The four-vectors of the pions are recalculated with an electron mass hypothesis and are afterwards combined. The resulting invariant mass must lie within $[2.8; 3.2]$ GeV/c^2, corresponding to the J/ψ signal region. Another two data samples are created with the combined invariant mass between $[2.4; 2.8]$ GeV/c^2 and $[3.2; 3.6]$ GeV/c^2, respectively, corresponding to the sideband regions below and above the J/ψ signal region.
10 million events have been generated for each of the three described mass regions at a beam momentum of $p_{\bar{p}} = 8.6819$ GeV/c.
The $p\bar{p} \to J/\psi\eta, J/\psi \to e^+e^-$ analysis module is run against the reconstructed $\eta\pi\pi$ data. The number of reconstructed entries in the signal region in dependence of the electron PID criteria is shown in Table 17.

In Fig. 13 the resulting reconstructed $J/\psi\eta$ mass is shown after applying all cuts for events from the J/ψ signal region. No pid requirements have been applied on the false electron candidates. About 200000 candidates are left out of 10 Million. For events from the J/ψ sideband regions, there are no candidates left after applying the same selection criteria. Fig. 15 shows the reconstruction efficiency on

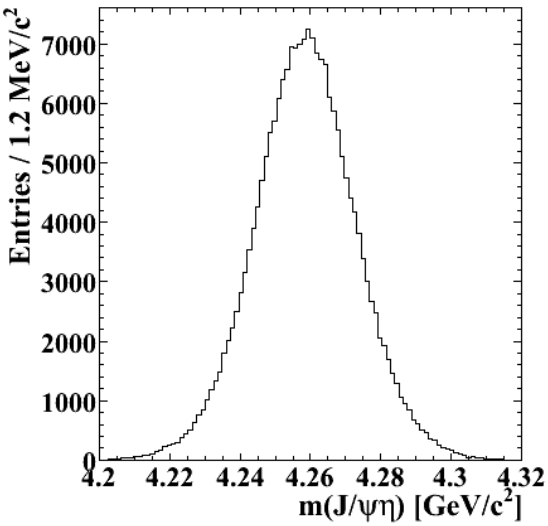

Figure 13: Reconstructed $J/\psi\eta$ mass from the background mode $\pi\pi\eta$, with the $\pi^+\pi^-$ mass (under electron mass hypothesis) within the J/ψ signal region.

the truth level.
In summary, one can limit the production to events whose generated $\pi\pi$ mass under electron mass hypothesis lies in the vivinity of the J/ψ mass. With a filter efficiency of 14%, the production time can be reduced by a factor of 7.

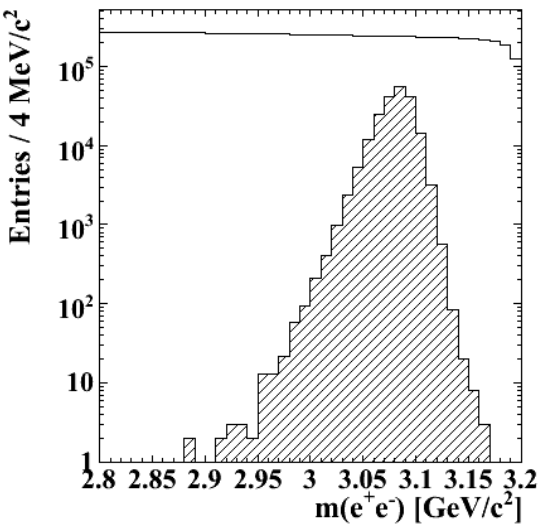

Figure 14: e^+e^- mass distribution (truth mass) before and after (cross-hatched) applying all cuts on the reconstructed data.

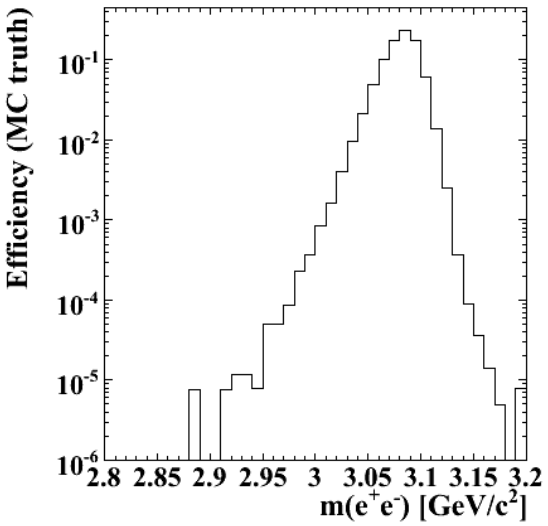

Figure 15: Reconstruction efficiency for wrongly identified e^+e^- pairs (truth mass).